Isotope ratio precision with transient sample introduction using ICP orthogonal acceleration time-of-flight mass spectrometry

Willie, S. N.; Mester, Z.; Sturgeon, R.

Publisher's version / Version de l'éditeur:
https://doi.org/10.1039/b505309a
Journal of Analytical Atomic Spectrometry, 20, 12, pp. 1358-1364, 2005

ARTICLE

JAAS
www.rsc.org/jaas

Isotope ratio precision with transient sample introduction using ICP orthogonal acceleration time-of-flight mass spectrometry

Scott Willie,* Zoltán Mester and Ralph E. Sturgeon

Institute for National Measurement Standards, National Research Council Canada, Ottawa, Ontario, Canada K1A 0R6

Received 15th April 2005, Accepted 27th September 2005
First published as an Advance Article on the web 21st October 2005

An assessment of inductively coupled plasma orthogonal acceleration time-of-flight mass spectrometry (ICP-*oa*-TOF-MS) for measurement of isotope ratios arising from steady-state and transient signal detection is presented. An HPLC pump and autosampler were used to introduce microliter volumes of analyte solution into a carrier flow to generate precise and repeatable transient signals having a FWHM of approximately 1 s. Analog and pseudo pulse data processing modes were evaluated and found to obey Poisson statistics for prediction of isotope ratio performance. Use of pseudo pulse counting is restricted by the limited linear range of response and cannot exceed approximately 0.2 counts per pushout. This limitation does not impede analog detection, which thus permits precise isotope ratio measurements to be achieved at higher analyte concentrations using shorter integration times. For transient signals, area measurements are superior to averaging point-to-point measurements across the peak for optimum ratio precision. Although the TOF system provides for simultaneous sampling of the extracted pulse, thereby permitting elimination of correlated noise through ratioing techniques, detection remains sequential and noise components present in the detection system limit isotope ratio precision in this study to 0.04% RSD.

Introduction

Inductively coupled plasma mass spectrometry (ICP-MS) is a principle technique for inorganic analytical laboratories, permitting application of various calibration strategies, including isotope dilution as a primary method of analysis. Currently, the most popular instruments use a scanning quadrupole mass filter (QMS) to separate ions of different mass/charge; however, there has been recent interest in time-of-flight (TOF) based detection. Reviews by Guilhaus[1,2] and Ray and Hieftje[3] discuss the advantages and difficulties of coupling a plasma source to a TOF-MS analyzer.

The basic principle of a TOF instrument is to electrostatically inject an isokinetic packet of ions into a flight tube which is either orthogonally or axially positioned relative to the source. Their subsequent drift permits separation as a result of their different velocities. The arrival time of an ion at the detector distinguishes its mass/charge. This requires a detector and processing electronics capable of recording events on a nanosecond time-scale with repetition rates, as each packet of ions is sampled, on the order of tens of microseconds. The analytical characteristics of an ICP-TOF-MS instrument produced by LECO (Renaissance) and based on axial acceleration (*aa*) have been presented in several reports.[4–6] Orthogonal acceleration (*oa*), used in the GBC OptiMass 8000 ICP-TOF-MS, has also been discussed.[7] The fundamental aspects of the two configurations have been contrasted in several reviews.[1–3,8,9]

The general advantages often cited with a TOF configuration include: (1) enhanced sample throughput and elemental coverage, wherein a complete mass spectrum is generated from each ion-gating event; (2) unlimited use of internal standards without performance compromises; (3) improved isotope ratio precision capability owing to the high correlation of the noise sources for all isotopes achieved with simultaneous sampling (extraction) and (4) elimination of time (spectral) skew to permit reliable characterization of multi-isotope signals arising from transient sample introduction devices such as laser ablation, flow injection, electrothermal vaporization and chromatographic based techniques.

Limitations to the accurate determination of multiple elements with fast transient signals using spectral scanning MS detectors have been the subject of several recent papers.[10–12] It has been argued that the nature of scanning instruments is not optimal for such multi-element measurements; as the number of ions of interest increase, the dwell time for each isotope decreases in order to preserve temporal signal information. As well, fluctuations in the rate of sample introduction and plasma noise restrict high precision isotope ratio measurement capability.

Resano *et al.*[11] have suggested that for a peak width of 1.5–2 s, three or four data points are sufficient to define transient signal profiles, permitting more than 20 elements to be determined using a QMS before detrimental effects on the precision, detection limits and sensitivity occur. By contrast, Björn *et al.*[12] have suggested that to obtain calibration slopes with less than 1% standard deviation it is necessary to acquire 7 to 24 data points to characterize a typical ETV peak using a 5 to 50 ms dwell time. This would limit the number of mass-to-charge ratios that could be monitored to between 4 and 10 with QMS detection. Irrespective of such arguments, the use of TOF based detection is an attractive approach to overcome such difficulties and has been pursued in a number of publications.[13,14] Peláez *et al.*[15] compared ICP-QMS and ICP-*aa*-TOF-MS for isotope ratio measurement precision on transients having different full width at half maximum (FWHM) characteristics. They recommended the TOF for peaks narrower than 8 s FWHM or when greater than 15 isotopes were to be measured. Wehmeier *et al.*[16] investigated the influence on precision and accuracy of isotope ratio measurements using different methods of peak calculation to characterize transient signals. Multi-collector ICP-MS and ICP-*aa*-TOF-MS were compared using point to point, area and trapezium methods for the determination of the $^{123/121}$Sb ratio. Carrión *et al.*[17]

DOI: 10.1039/b505309a

concluded that acquisition times should be as long as possible while maintaining good transient peak definition for the best precision on isotope ratios measured with transients. However, it should be noted that in their study signal profiles similar to those obtained by laser ablation (LA), which can approach 1 min FWHM, were considered to be "transient".

The application of ICP-*oa*-TOF-MS to the measurement of precise multi-isotope ratios derived from transient signals is the primary subject of this study wherein consideration is given to the fundamental limitations of the detection system and counting statistics that ultimately impact resulting performance. Based on knowledge of these limitations, experiments can be designed to derive the maximum possible performance from such an instrument.

Experimental

Instrumentation

An OptiMass 8000 ICP-*oa*-TOF-MS instrument (GBC Scientic Equipment Pty. Ltd, Australia) was used. Since the publication of ref. 7, the data acquisition components of the OptiMass 8000 have been upgraded to incorporate a digital signal averager (Model: AP100, Acqiris, Geneva, Switzerland). The averager is capable of operating at 1 gigasample per second (GS s^{-1}) but is set to 0.5 GS s^{-1} to provide a sampling interval of 2 ns. This sampling rate is used to ensure a compatible transfer rate, up to 100 MB s^{-1} (using PCI bus) to the PC. The averager has a 500 MHz analog bandwidth and 8 bits of vertical resolution. The sustained trigger rate of the digitizer can easily keep up with the typical cycle times of the OptiMass without data loss. No on-board data processing was performed before data transfer.

Ion detection was achieved utilizing a discrete dynode electron multiplier (Model AF834H, ETP, Ermington, NSW, Australia). Data was compiled by Microsoft Access software and subsequently exported to Microsoft Excel spreadsheets for further manipulation. Instrument conditions were optimized daily for ^{165}Ho response with respect to both peak height sensitivity and peak shape (resolution). Typical instrument settings are summarized in Table 1. No mass bias corrections were applied in these experiments. Samples were introduced using a concentric nebulizer (Glass Expansion Pty. Ltd, Camberwell, Victoria, Australia) coupled to a 50 ml thermostated (15 °C) cyclonic spray chamber (Glass Expansion). Transient sample introduction was performed using an Agilent 1100 binary HPLC pump and autosampler (Agilent Technologies Inc., Palo Alto, CA).

Table 1 ICP-TOFMS operating conditions

ICP source:	
Rf power (27.12 MHz)	1150 W
Plasma gas flow rate	10 l min^{-1}
Auxiliary gas flow rate	1.0 l min^{-1}
Nebulizer gas flow rate	0.920 l min^{-1}
Mass spectrometer:	
Ion optics	
Skimmer	−900 V
Extraction	−1300 V
Z1	−90 V
Y mean	−50 V
Y deflection	−4 V
Z lens mean	−1200 V
Z lens deflection	0 V
Lens body	−145 V
Pulse shaping:	
Fill	−32 V
Fill bias	0.5 V
Fill grid	−19 V
Pushout plate	605 V
Pushout grid	−440 V
Reflectron	680 V
Detection:	
Multiplier gain:	2300 V

Procedure

Both steady-state and transient sample introduction were studied. Various acquisition times were evaluated, as were the effects of analyte concentration and isotope abundance. For steady-state measurements, liquid uptake rate was controlled by selection of the instrument peristaltic (12 roller) pump speed and set for approximately 1.2 ml min^{-1}.

To simulate transient signals, the HPLC pump was connected to the nebulizer using 0.02″ (id) Teflon tubing and operated at 3 ml min^{-1} using deionized water (DIW) as a carrier. Sample injection volumes of 2 μL were used. Reproducibility of sample introduction was assessed using the Agilent UV detector and found to conform with the manufacturer specifications of <1% RSD for repeat measurements.

Reagents and standards

Deionized water (DIW) was obtained from a NanoPure (Barnsted, UK) purification system using reverse osmosis water as a feed. High purity HNO_3 was prepared in-house by sub-boiling distillation of the reagent grade feedstock using a quartz still housed in a Class 10 fume cupboard. Stock solutions of the various elements were prepared by dissolution of the pure elements or their high-purity salts (Alfa Aesar, Ward Hill, MA) in acid, followed by dilution with DIW and storage in pre-cleaned screw capped polypropylene bottles.

Results and discussion

The effects of drift and multiplicative noise from the ICP can contribute to imprecision when measuring isotope ratios. Consequently, careful optimization of the peak hopping approach used to quantitate signals with QMS based instruments is required to minimize the effects of these noise sources. In QMS systems, the mass filter is tuned to the mass of interest, the electronics are allowed to settle and the measurement is taken for a fixed period of time (*i.e.*, dwell time). The process is repeated sequentially for each m/z over the selected acquisition time. As more isotopes are included in the suite of analytes to be determined, the measurement precision can further deteriorate as decreased time is spent acquiring ion intensity for a particular isotope. This problem can be minimized (but not eliminated) with steady-state sample introduction by employing acquisition times of several minutes. However, for transient signals that evolve over a period of a few seconds, measurement time is limited and this option is not available.

One of the benefits often cited with TOF based instrumentation is that the entire mass range can be sampled in a short period of time such that source noise is essentially eliminated from the final measurement.[6] The GBC OptiMass 8000 samples the continuous ion beam by an electrostatic orthogonal pushout of a discrete volume of ions. This packet of ions is then m/z separated in a 0.7 m flight tube equipped with a reflectron (providing an effective 1.4 m overall flight path), where the heaviest ion of interest (260 u) takes approximately 32 μs to reach the detector. The pushout frequency for each ion packet is 29411 Hz or every 34 μs. During the selected acquisition time the signal is summed over the corresponding number of pushouts. For example, 147 055 pushouts are summed during a 5 s acquisition time and 2941 pushouts for a 0.1 s period. Since each pushout reflects simultaneous multi-element coverage,

noise sources in the plasma uniformly influence the signal over the mass range, unlike sequential peak hopping measurements where rapid fluctuations can affect signals unequally. Thus, correlated noise related to ion extraction can be eliminated using ion ratioing techniques. However, ion detection using a TOF-MS occurs in a sequential fashion and noise that affects the analyzer and detection portion of the instrument cannot be eliminated in this manner.

It is an often stated advantage of the TOF that it has the ability to generate an entire mass spectrum for each repetition or *oa* pushout.[9] Although true, in practice the signals recorded from one *oa* pulse are often too small to be useful, as the peaks are imprecisely defined and insufficient number of ions are collected to have any statistical relevance. Accurate spectra are created from histogrammed counts of ion arrival events over several thousand individual *oa* pushouts. Monitoring of single pushouts was pursued in this study in an attempt to gain an understanding of the signal processing characteristics of this instrument.

Signal processing

A prerequisite of TOF-MS is the ability to digitize very fast signals over a useful dynamic range. Two modes of signal processing, analog and pseudo-pulse counting, are available and are described below.

Analog mode

In analog mode, the discrete dynode electron multiplier detector responds to an ion arrival event with production of a 3–5 ns wide pulse of electrons having an amplitude proportional to the number of ions striking the detector. This electron current is converted to a voltage and subsequently amplified and processed by the signal averager to produce a digitized output. Analog outputs are typically measured in volts, although the term counts (as designated by the instrument software) will be used in all subsequent discussion. The AP100 resolves the input into 256 voltage levels that correspond to the 8-bit ADC range of 0 to 255 "counts". The voltage corresponding to zero counts is determined by a voltage offset value from a baseline measurement. The ion signals are assigned to sequential 2 ns time bins covering the mass range up to 260 u. Since the time width of a single ion peak can vary, and is generally greater than 2 ns, it is typical that signals are collected in 3 to 5 time bins around the centroid of the mass peak. The digital averager sums the results for each specific 2 ns time bin for every pushout over the acquisition period specified.

Steady-state sample introduction was initially used to evaluate the characteristics of the detector for recording each *oa* pushout. The amplitude of the output pulse from a single ion striking the detector is not of fixed magnitude, but follows a distribution of pulse heights. Fig. 1 displays the pulse height distribution of the signal obtained for the introduction of a 0.5 ng ml^{-1} solution of Ho. These results were generated by monitoring 29 time bins centered on m/z 165 with an acquisition time of 34 μs (*i.e.*, a single *oa* pushout); 1000 sequential pushouts were recorded. Ion arrival event "signals" were found in 101 of the 1000 pushouts collected. One pushout contained an output of 74 "counts" summed over the 29 time bins, although 6 and 18 counts were the most frequently recorded signal intensities. Based on a consideration of the Poisson distribution, it can be calculated that the probability of more than one ion being responsible for the signal in a particular time bin is only 0.5%. Fig. 1 presents the case of a weak signal wherein noise from the amplifier electronics results in a significant FWHM of the pulse height distribution. For this example, the peak threshold for the detector was set at five and thus pushouts generating one to four unit "counts" were ignored.

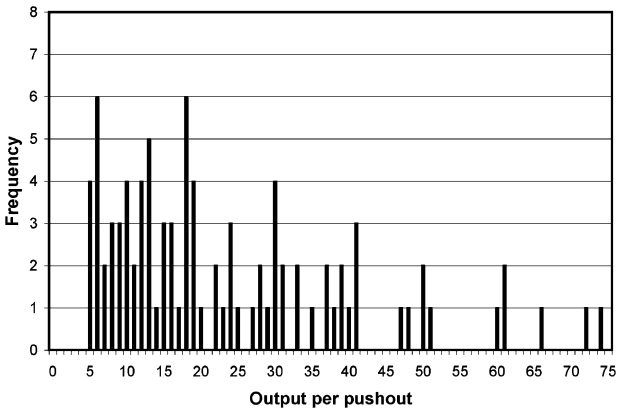

Fig. 1 Detector output in analog mode representing distribution of pulse heights obtained for 1000 pushouts during steady-state introduction of a 0.5 ng ml^{-1} solution of ^{165}Ho.

Pseudo pulse mode

The data acquisition system can be used in a pseudo pulse counting mode, wherein the signal averager operates in a binary fashion, limiting the output to a maximum of one count per event. In other words, instead of the measurement of multiple counts over consecutive time bins, some that could be as large as 74 (Fig. 1), only one count or output signal is registered to a single time bin. This is a function of the signal averager and hence the term "pseudo pulse" is appropriate as this approximates pulse counting but is not in the conventional sense a pulse counter. It should be reiterated that the use of the term "counts" as signal units may mislead readers, as it is used in both analog and pseudo pulse modes. In pseudo pulse mode, introduction of a 0.5 ppb solution of Ho resulted in 101 counts, one for every ion arrival event, whereas with analog recording, the same solution produced an output of 2205 (*i.e.*, summed counts in Fig. 1). Pseudo pulse counting severely limits the linear response of the detection system, as multiple ions of a given m/z arriving at the detector result in only one count being registered. As well, in pseudo pulse counting mode the apparent peak resolution is slightly improved for the same number of ion arrival events. With analog counting, a signal above the threshold is registered over several consecutive times bins which are then summed over multiple pushouts to define the peak shape. With pseudo pulse measurements, the signal from an ion event is assigned to only one 2 ns time bin at the centroid of the analog pulse. Consequently, the resulting peak, derived by summing many ion arrival events, is more narrow in pseudo pulse than analog acquisition mode as the later reflects not only the ion arrival time at the detector but also the width of the resulting impulse.

Limitations of linear range

Linearity in pseudo-pulse mode was assessed by preparing a graph of counts per pushout *vs.* analyte concentration. For this purpose, a selection of isotopes was used to construct calibration curves over the range from 0 to 20 ng ml^{-1}. The output from each pushout was recorded. The baseline mass width of the m/z range integrated was dependent on the isotope, but was generally 0.7 to 0.8 u centered on the m/z of interest. Results are presented in Fig. 2, wherein deviation from linearity is observed to occur in the range of 0.2 counts per pushout for all isotopes. This fundamental limitation to linear range with this instrument is independent of the sensitivity. In the case of ^{103}Rh, this corresponds to a concentration of approximately 2 ng ml^{-1}. Clearly, a 10-fold more sensitive instrument will attain non-linear response at a 10-fold lower concentration.

In analog mode, calibration linearity is not similarly restricted. As previously noted, many counts per pushout can be

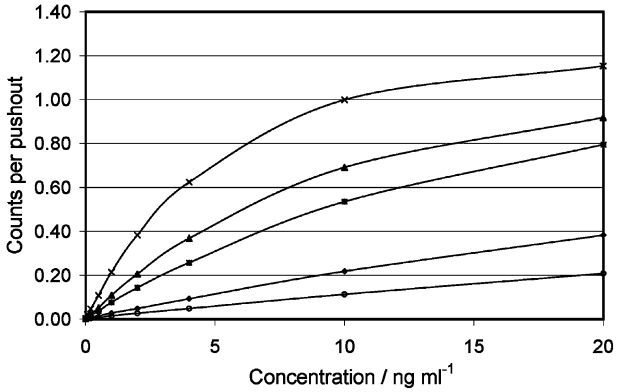

Fig. 2 Counts per pushout *vs.* concentration. ○ ^{65}Cu, ◇ ^{63}Cu, ■ ^{173}Yb, ▲^{102}Rh, × ^{238}U.

recorded, contrary to the limitation of one count per pushout in pseudo pulse mode. The upper limit of linearity in analog mode occurs near 500 ng ml^{-1}. Fig. 3 displays calibration curves for ^{107}Ag using both measurement methods. In this case, the analog signal output was 50-fold larger than the pseudo pulse signal in the concentration range where both systems have a linear response. The exact cross-calibration factor is detector voltage dependent, the analog signal approximately doubles with every increase in 100 V applied to the detector whereas the pseudo pulse signal remains relatively constant, as would be expected since only the first bit of the ADC is used.

Poisson counting statistics

Steady-state measurements. For detection systems which respond to the random arrival of counted entities, Poisson counting statistics dictates that the precision of such measurements is proportional to the square root of their signal intensity (number of ion counts). Experimentally, response from the pseudo pulse mode is found to be in accord with this principle; measurement precision follows a parabolic decay with increasing count rate, approaching an asymptotic value at high signal intensity. As an example, the precision of measurement of the $^{107/109}$Ag ratio, expressed as an RSD, is presented in Fig. 4 and compared to theoretical values for acquisition times varying from 0.05 to 500 s. A 2 ppb solution was used to derive these data as this concentration is at the upper limit of linearity for pseudo pulse mode data acquisition. A limiting precision of 0.04% RSD is achieved, comparable to values reported previously with ICP-*aa*-TOF-MS.[4,6]

Fig. 4 also displays results obtained with analog signal processing. The precision of analog measurements cannot be predicted without first converting the analog intensities to their

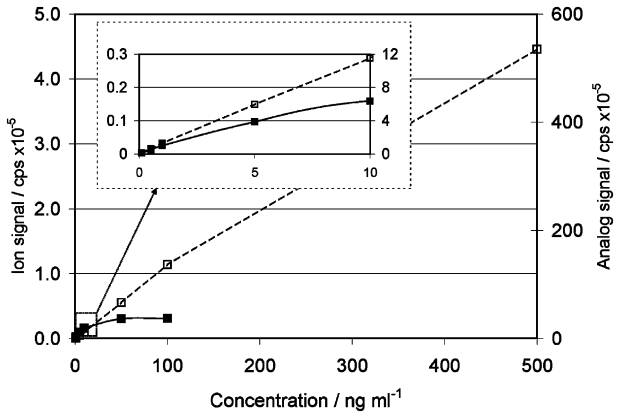

Fig. 3 Calibration curve for ^{107}Ag using — pseudo pulse and -- analog detection.

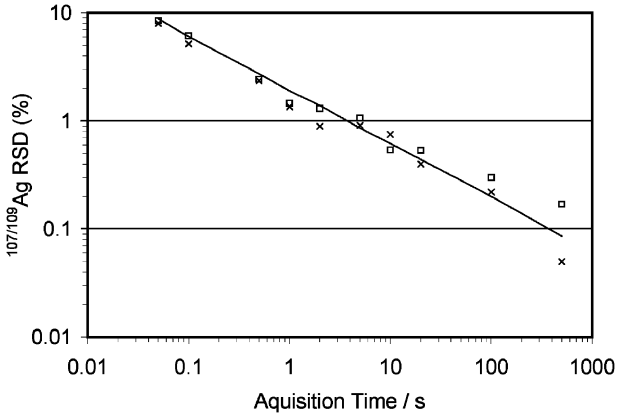

Fig. 4 Effect of acquisition time on $^{107/109}$Ag ratio precision. 2 ng ml^{-1}, □ measured analog counting, × measured pseudo pulse counting, — Poisson statistics based on measured pseudo pulse response.

equivalent pseudo pulse response using the cross-correlation conversion factor. The precision of the converted analog signals agrees quite well with the pseudo pulse and theoretical precision for the same acquisition times.

The precision of the $^{107/109}$Ag ratio in analog mode was further examined by constructing a calibration curve up to 1000 ng ml^{-1}, well beyond the pseudo pulse linearity limit of 2 ppb. Again, converting the analog response to equivalent pseudo pulse values provided RSD's in good agreement with calculated theoretical values, as shown in Fig. 5. Data are based on the mean of seven repeats of a series of Ag calibration solutions.

Isotope ratio performance for transient sample introduction

Point-to-point measurement. Several choices are available when isotope ratio measurements are to be derived from transient signals. The time integrated peak area or peak height of the transient as well as the individual points that define the transient can all be used to calculate such ratios. One obvious criterion when taking ratio measurements from disparate signal intensities is that linear response is essential. If the signal of the most abundant isotope begins to deviate from linearity before that of the less abundant isotope, inaccurate ratios will occur. An example of this is shown in Fig. 6A, which displays a transient signal for Tl. The $^{205/203}$Tl ratio changes continuously over the peak profile as the signals for ^{205}Tl and ^{203}Tl are not linearly related to each other over the full portion of the transient; as signal saturation is evident over the peak of the ^{205}Tl signal. In analog mode, the same solution produced the transient shown in Fig. 6B. A constant $^{205/203}$Tl ratio is evident

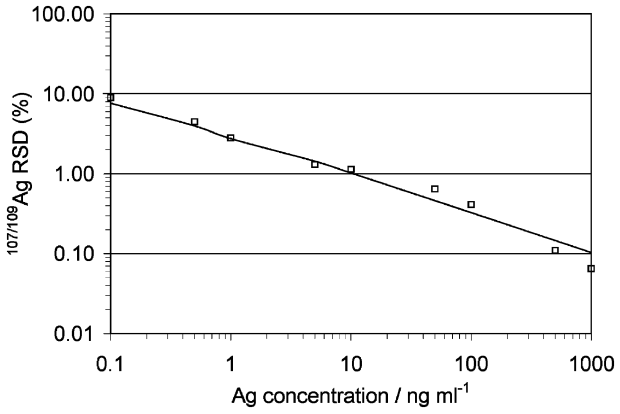

Fig. 5 RSD of $^{107/109}$Ag ratio *versus* concentration for 1 s integration, $n = 7$. □ measured analog counting, — Poisson limit based on conversion of intensity of equivalent pseudo pulse mode results.

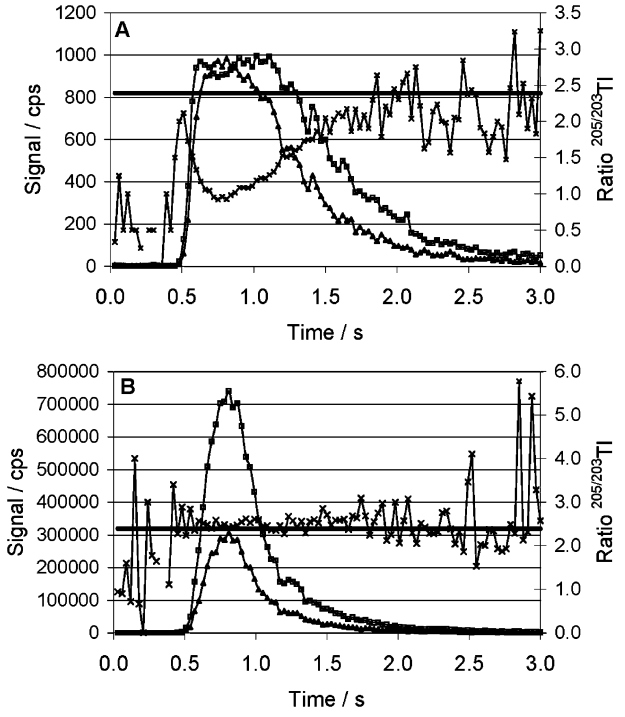

Fig. 6 Transient response for HPLC introduction of 1 μl of 10 μg ml^{-1} Tl. □ ^{205}Tl, ▲ ^{203}Tl, × $^{205/203}Tl$, — expected ratio. A pseudo-pulse, B analog.

over the peak FWHM that gradually becomes limited by signal noise at the extremes of the transient.

Peak area measurement. Isotope ratios can also be calculated using total time integrated peak area intensities if resolution is sufficient that overlap from adjacent peaks is not an issue. Transient peaks were generated using an HPLC pump to introduce discrete 2 μl volumes of a multielement solution into a 3 ml min^{-1} flow of DIW. These signals are temporally similar to those generated using ETV sample introduction and were used for the calculations that follow.

A selection of seven isotope ratios ranging from 1 : 1 ($^{142/144}Nd$) to 1 : 46 ($^{208/204}Pb$) was measured with the maximum count rate for the most abundant isotope designed to be near the upper range of linear calibration response (in pseudo pulse mode) so as to guarantee optimum precision. Using pseudo pulse counting, acquisition times over the 3 s of measurement time were varied between 10 and 1000 ms. Table 2 summarizes the theoretical RSDs for the various ratio measurements and compares them to the experimental RSD of the mean derived from seven injections. As the isotope abundance becomes more divergent, the RSD generally increases as the response from the lesser abundant isotope approaches the baseline noise. Random variation is observed in the determined RSD's for a specific ratio as the acquisition time changes, suggesting that the number of points used to define the peak is not an important factor when the entire peak area is used for this calculation and there is otherwise no interest in the temporal information associated with the peak. The same experiment was performed using analog detection. Consistent with previous results, the RSD's obtained were similar to the pseudo-pulse counting results shown in Table 2.

Two different calculations (total area and average of point-to-point measurements across the peak) were compared for the calculation of ratios using analog recording. The results for the point-to-point method are summarized in Table 3, based on seven repeat transients. The points included in the calculation of the mean were chosen to be those above the FWHM of the peak. The individual data points defining the isotope pairs for each transient were ratioed and the mean of the calculated ratios was taken. These values were then used to calculate the standard deviation of the mean for the seven repeat transients. The results in Table 3 show that the precision of the ratio measurement is degraded as more data points are used to define the transient because the associated shorter acquisition periods result in lower intensities for each measurement and correspondingly less precise ratios, in accordance with Poisson statistics.

Table 4 illustrates the situation wherein the isotope ratios are calculated from the time integrated area of the entire transient. Results are reported as the standard deviation of the mean of seven repeats. The ratios are generally more uniform for the various acquisition times compared to the point-to-point results. As expected, the precision degrades as more disparate ratios are measured and the signal for the less abundant isotope decreases.

It should be noted that the data presented in Tables 3 and 4 are based on measurements of small signal transients (120 pg absolute) and chosen to enable comparison with pseudo pulse data collection. Isotope ratio reproducibility is significantly improved when more intense signals are processed. As shown by several authors,[6,18] the level of precision that can be attained in such case is comparable to that currently available with most quadrupole based instruments, *i.e.*, 0.04%.

When multiple isotopes are to be measured, the superior sensitivity of quadrupole based instruments can offset the benefits obtained from simultaneous based detection systems when data are primarily count rate limited. Individual situations will dictate the extent of this advantage. When transients are measured, advantages in sensitivity can be further offset by the number of data points that must be acquired in order to accurately sample the peak in time. As previously noted, however, with TOF based detection the number of points used to define a transient peak is not an important factor when the entire peak area is used for quantitation.

For steady-state measurements, a recent example illustrating the benefit of the simultaneous measurement capability of the

Table 2 Effect of acquisition time on isotope ratio precision derived from transient signals recorded in pseudo pulse counting mode using peak area intensity

		Precision of measurement, RSD, %								
			Acquisition times, ms							
Element	Expected ratio	Theoretical	1000	500	200	100	50	40	20	10
$^{142/144}Nd$	1.14	3.6	3.1	4.7	2.8	5.0	4.2	3.6	3.1	2.9
$^{174/173}Yb$	1.97	3.4	2.4	3.0	3.3	2.4	1.2	4.0	3.1	2.8
$^{142/145}Nd$	3.27	5.2	3.4	6.1	8.1	5.8	4.9	3.7	4.3	5.8
$^{142/148}Nd$	4.71	5.8	9.2	6.1	3.0	5.6	6.3	8.8	4.3	7.4
$^{174/170}Yb$	10.4	6.7	5.7	5.5	4.4	4.9	5.8	5.7	4.0	3.7
$^{115/113}In$	22.3	10.6	11.1	9.0	5.8	12.0	10.0	8.3	10.0	8.4
$^{208/204}Pb$	46	11.2	5.4	12.3	6.3	11.4	5.8	13.4	14.4	8.0

Table 3 Effect of acquisition time on isotope ratios and their precision of measurement derived from transient signals recorded in analog mode using point-to-point calculations across the peak[a]

		Acquisition time, ms							
		10		20		40		100	
		30 data points[b]		15 data points		10 data points		5 data points	
Element	Expected ratio	Ratio	SD	Ratio	SD	Ratio	SD	Ratio	SD
$^{142/144}$Nd	1.14	1.23	0.05	1.13	0.01	1.11	0.03	1.10	0.03
$^{174/173}$Yb	1.97	2.26	0.09	2.09	0.07	2.14	0.04	2.12	0.05
$^{142/145}$Nd	3.27	4.54	0.26	3.36	0.14	3.34	0.13	3.34	0.06
$^{142/148}$Nd	4.71	5.49	0.30	4.97	0.11	5.00	0.26	4.61	0.20
$^{174/170}$Yb	10.43	22.14	3.40	13.86	0.41	12.86	0.57	13.16	0.52
$^{115/113}$In	22.31	37.19	3.87	35.45	3.52	42.67	9.36	32.73	3.81

[a] Mean and standard deviation of the mean, $n = 7$. [b] Number of data points above the FWHM of the peak.

Table 4 Effect of acquisition time on isotope ratios and their precision of measurement derived from transient signals recorded in analog mode using peak area calculations[a]

		Acquisition time, ms							
		10		20		40		100	
Element	Expected ratio	Ratio	SD	Ratio	SD	Ratio	SD	Ratio	SD
$^{142/144}$Nd	1.14	1.08	0.06	1.11	0.02	1.09	0.07	1.09	0.05
$^{174/173}$Yb	1.97	2.12	0.06	2.04	0.09	2.12	0.06	2.07	0.12
$^{142/145}$Nd	3.27	3.29	0.39	3.15	0.22	3.13	0.23	3.27	0.21
$^{142/148}$Nd	4.71	4.54	0.41	4.43	0.19	4.74	0.47	4.47	0.46
$^{174/170}$Yb	10.43	11.6	1.1	11.2	0.26	11.8	0.92	12.1	0.85
$^{115/113}$In	22.31	24.2	3.9	21.2	2.9	21.8	3.2	26.6	4.4

[a] Mean and standard deviation, $n = 7$.

TOF was demonstrated by Yang *et al.*[19] For the measurement of three isotopes of Hg, the augmented noise from the sample introduction system incorporating a gas liquid separator does not limit the precision obtained using the TOF, whereas this noise source remains a significant factor for a scanning based detection system.

Conclusions

An understanding of the characteristics and limitations of the detection modes available with the OptiMass 8000 ICP-*oa*-TOF-MS enables users to select and optimize measurement protocols to fit their analytical requirements. Precision of isotope ratio measurements with this instrument is generally dictated by Poisson counting statistics, both for steady-state and transient sample introduction.

As with all detection systems used for simultaneous or sequential isotope ratio determinations, linearity in measurement must be assured, otherwise accuracy is forfeited. When using (pseudo) pulse counting for *oa*-TOF-MS characterization of transient signals, this limits ion flux to the detector to <0.2 ions per pushout. Enhancing the ion yield or sensitivity of the instrument will not serve to remove this limitation, which is inherent to this pseudo pulse counting detection system. Isotope ratio precision can, of course, be enhanced by time integrating the total counts under the signal transient or by summing results (*i.e.*, integrated counts) arising from introduction of replicate transients so as to improve counting statistics derived from a mean of several measurements.

Analog measurement mode is thus preferable, and ratio precision can be circuitously predicted from the relationship between pseudo pulse counting and analog output (*i.e.*, the cross-correlation factor), as it also obeys Poisson statistics. However, because the constraint of maintaining ion arrival events at <0.2 per pushout is no longer present, higher analyte concentrations can be tolerated (while maintaining linearity of response), thereby enhancing precision by acquisition of increased counts at both the peak apex and over the area of a transient signal. Under steady-state conditions, a count limited precision of 0.04% for the 107/109Ag ratio was obtained using a 20 s acquisition and introduction of a 200 ppb solution. This limit is comparable to data reported in other studies using ICP-TOF-MS.[4,6] Attempts to further enhance isotope ratio precision using increased integration times or higher analyte concentrations were unsuccessful. Clearly, there are additional sources of non-correlated noise arising from the detection system. One of which may be related to the ion pulse height distribution. Similarly, at extremely low concentrations (approaching the detection limit), isotope ratio precision likely again deviates from a predictable Poisson statistic because noise arising from the ion pulse height distribution again becomes the major noise source. This aspect was not investigated here, as the objective was to optimize conditions under which the most precise measurements could be achieved.

References

1 M. Guilhaus, *Spectrochim. Acta, Part B*, 2000, **55**, 1511–1525.
2 M. Guilhaus, D. Selby and V. Mlynski, *Mass Spectrom. Rev.*, 2000, **19**, 65–107.
3 S. J. Ray and G. M. Hieftje, *J. Anal. At. Spectrom.*, 2001, **16**, 1206–1216.
4 F. Vanhaecke, L. Moens, R. Dams, L. Allen and S. Georgitis, *Anal. Chem.*, 1999, **71**, 3297–3303.
5 X. Tian, H. Emteborg and F. C. Adams, *J. Anal. At. Spectrom.*, 1999, **14**, 1807–1814.
6 H. Emteborg, X. Tian, M. Ostermann, M. Berglund and F. C. Adams, *J. Anal. At. Spectrom.*, 2000, **15**, 239–246.
7 R. E. Sturgeon, J. W. H. Lam and A. Saint, *J. Anal. At. Spectrom.*, 2000, **15**, 607–616.

8 M. Guilhaus, V. Mlynski and D. Selby, *Rapid Commun. Mass Spectrom.*, 1997, **11**, 951–962.
9 G. M. Hieftje, D. P. Myers, G. Li, P. P. Mahoney, T. W. Burgoyne, S. J. Ray and J. P. Guzowski, *J. Anal. At. Spectrom.*, 1997, **12**, 287–292.
10 J. D. Venable, D. Langer and J. A. Holcombe, *Anal. Chem.*, 2002, **74**, 3744–3753.
11 M. Resano, M. Verstraete, F. Vanhaecke and L. Moens, *J. Anal. At. Spectrom.*, 2001, **16**, 1018–1027.
12 E. Björn, D. C. Baxter and W. Frech, *J. Anal. At. Spectrom.*, 2002, **17**, 1582–1588.
13 P. P. Mahoney, S. J. Ray, G. Li and G. M. Hieftje, *Anal. Chem.*, 1999, **71**, 1378–1383.
14 G. Centineo, M. Montes Bayón and A. Sanz-Medel, *J. Anal. At. Spectrom.*, 2000, **15**, 1357–1362.
15 M. V. Peláez, J. M. Costa-Fernández and A. Sanz-Medel, *J. Anal. At. Spectrom.*, 2002, **17**, 950–957.
16 S. Wehmeier, R. Ellam and J. Feldmann, *J. Anal. At. Spectrom.*, 2003, **18**, 1001–1007.
17 M. Castillo Carrión, J. Reyes Andrés, J. Antonio Martín Rubí and H. Emteborg, *J. Anal. At. Spectrom.*, 2003, **18**, 437–443.
18 H. P. Longerich and W. Diegor, *J. Anal. At. Spectrom.*, 2001, **16**, 1196–1201.
19 L. Yang, S. Willie and R. E. Sturgeon, *J. Anal. At. Spectrom.*, 2005, **20**, 1226–1231.